arXiv:1411.5975v2 [astro-ph.SR] 24 Apr 2015

Analysis of Late–time Light Curves of Type IIb, Ib and Ic Supernovae

J. Craig Wheeler[1], V. Johnson[1], A. Clocchiatti[2]

wheel@astro.as.utexas.edu

ABSTRACT

The shape of the light curve peak of radioactive–powered core–collapse "stripped–envelope" supernovae constrains the ejecta mass, nickel mass, and kinetic energy by the brightness and diffusion time for a given opacity and observed expansion velocity. Late–time light curves give constraints on the ejecta mass and energy, given the gamma–ray opacity. Previous work has shown that the principal light curve peaks for SN IIb with small amounts of hydrogen and for hydrogen/helium–deficient SN Ib/c are often rather similar near maximum light, suggesting similar ejecta masses and kinetic energies, but that late–time light curves show a wide dispersion, suggesting a dispersion in ejecta masses and kinetic energies. It was also shown that SN IIb and SN Ib/c can have very similar late–time light curves, but different ejecta velocities demanding significantly different ejecta masses and kinetic energies. We revisit these topics by collecting and analyzing well–sampled single–band and quasi–bolometric light curves from the literature. We find that the late–time light curves of stripped–envelope core–collapse supernovae are heterogeneous. We also show that the observed properties, the photospheric velocity at peak, the rise time, and the late decay time, can be used to determine the mean opacity appropriate to the peak. The opacity determined in this way is considerably smaller than common estimates. We discuss how the small effective opacity may result from recombination and asymmetries in the ejecta.

Subject headings: diffusion – opacity – radiative transfer – supernovae: general

[1]Department of Astronomy, University of Texas at Austin, Austin, TX, USA.

[2]Universidad Catolica, Chile

1. Introduction

Clocchiatti & Wheeler (1997) noted several apparent properties of "stripped–envelope" supernovae: (1) Some events completely trap gamma–rays for hundreds of days. The only known examples of these slow light curves were SN Ib. (2) Some events display a similar photometric evolution with an intermediate later time rate of decline, similar to SN 1993J, despite their spectral variety, SN IIb, SN Ib, SN Ic. (3) Some events decline especially rapidly from maximum, show an especially large peak to tail contrast, but show a slope comparable to those of the intermediate slope class (point 2) at very late times, over 100 d after maximum. These events all seemed to be SN Ic. Drout et al. (2011) found that the behavior of the light curve peaks of stripped–envelope events were rather similar, with SN Ib and SN Ic having statistically indistinguishable decline rates up to $\sim$ 40 d after maximum, implying similar ejecta mass and energy. Taddia et al. (2014) find that SN Ic and SN Ic–BL have shorter rise times than SN IIb and SN Ib, but that the immediate post–peak declines are similar for all categories. Similar decline rates shortly after peak, with some dispersion, were also noted by Cano (2013) and Lyman et al. (2014). This evidence for similar post–peak decline rates belies the long–standing evidence for late–time light curve dispersion. Here, we compile light curve data for late–time light curves of stripped–envelope supernovae and re-investigate the uniformity of the late–time behavior. We concentrate here on light curve properties. See Modjaz et al. (2014) for a recent compilation of spectral properties and Bianco et al. (2014) for a compilation of light curves. Section 2 defines the analytical basis of our analysis. Section 3 presents the data. Section 4 gives a discussion and Section 5 summarizes our conclusions.

2. Peaks and Tails

We analyze data from the literature on the light curves of stripped–envelope supernovae. We did our own compilation, but see Cano (2013) for an independent compilation, including some long–term data of the same events we present here. We estimate the ejecta mass and energy from the observed rise time and photospheric velocity near peak light, and an effective opacity, assumed to be constant. Following Arnett (1982) we write

$$M_{ej} \sim \frac{1}{2}\frac{\beta c}{\kappa} v_{ph} t_r^2 = 0.77\ M_\odot \left(\frac{\kappa}{0.1\ \mathrm{cm^2\ g^{-1}}}\right)^{-1} v_{ph,9} \left(\frac{t_r}{10\ d}\right)^2, \quad (1)$$

where $\beta = 13.8$ is an integration constant, c the speed of light, κ is the effective UVOIR opacity, v_{ph} is the velocity at the photosphere with $v_{ph,9}$ in units of 10^9 cm s^{-1}, and t_r the rise time to maximum light. This equation is based on assumptions of homologous expansion

and self–similar diffusion with a power source at the center of spherical ejecta. Two further assumptions are that v_{ph} is a reasonable proxy for the scaling velocity in the model and that the rise time to maximum light is a reasonable proxy for the effective timescale in the model, $t_{eff} = \sqrt{2t_d t_h}$, where t_d is the model diffusion time and t_h the model hydrodynamical time. In practice, the photospheric velocity will be affected by the distribution of density and opacity and hence may not precisely represent a fixed scaling velocity, the rise time is not exactly equal to t_{eff} even in the context of the basic model (Chatzopoulos et al. 2013), and the opacity will be constant neither in space nor time.

The corresponding kinetic energy is then

$$E_{ke} = \frac{1}{2} M_{ej} < v^2 >, \tag{2}$$

which implicitly defines the mean squared expansion velocity. This velocity cannot be measured directly, so a relation must be adopted between this velocity and the velocity at the photosphere. We adopt the relation for a constant density sphere, $< v^2 >= 3/5 v_{ph}^2$[1]. With this relation we can then write

$$E_{ke} = \frac{3}{10} M_{ej} v_{ph}^2 = \frac{3}{20} \frac{\beta c}{\kappa} v_{ph}^3 t_r^2 = 4.6 \times 10^{50} \text{ ergs} \left(\frac{\kappa}{0.1 \text{ cm}^2 \text{ g}^{-1}} \right)^{-1} v_{ph,9}^3 \left(\frac{t_r}{10 \ d} \right)^2, \tag{3}$$

so E_{ke} is proportional to v_{ph}^3 and hence sensitive to the choice of v_{ph} and its dispersion among events.

For the late-time tail, we adopt the formalism of Clocchiatti & Wheeler (1997) and define a characteristic timescale

$$T_0 = (\frac{C \kappa_\gamma M_{ej}^2}{E_{ke}})^{1/2}, \tag{4}$$

where C is a dimensionless structure constant dependent on the slope of the density profile and is typically C ~ 0.05, and κ_γ is the opacity to gamma rays. Using Equation (1) for M_{ej}, this can also be written

$$T_0 = \left[\left(\frac{5 \beta C}{3} \right) \left(\frac{c}{v} \right) \left(\frac{\kappa_\gamma}{\kappa} \right) \right]^{1/2} t_r = 32 \text{ d} \left(\frac{\kappa_\gamma / 0.03}{\kappa / 0.1} \right)^{1/2} v_{ph,9}^{-1/2} \left(\frac{t_r}{10 \ d} \right), \tag{5}$$

where we take as a fiducial optical opacity $\kappa = 0.1$ cm^2 g^{-1} and as a fiducial gamma–ray opacity $\kappa_\gamma = 0.03$ cm^2 g^{-1}.

---

[1]Note that there is a typo in Arnett (1982) where the relation between photospheric velocity, kinetic energy and mass is given as $v_{ph}^2 = 3/5(2E_{ke}/M_{ej})$. This error was corrected in Arnett (1996) where the correct relation is given, $v_{ph}^2 = 5/3(2E_{ke}/M_{ej})$, but the error has propagated in the literature in, among other works, Valenti et al. (2008a), Chatzopoulos, Wheeler & Vinko (2012) and Chatzopoulos et al. (2013) who wrote $M_{ej} \sim \frac{3}{10} \frac{\beta c}{\kappa} v t_r^2$ without carefully specifying the prescription for the velocity.

We take the radiated power to be

$$L_{in} = L_{decay}\left(1 - e^{-(T_0/t)^2}\right), \tag{6}$$

where L_{decay} is the total input from gamma–rays and positrons from the radioactive decay of ^{56}Ni and ^{56}Co according to

$$L_{decay} = A[e^{-t/t_{Ni}} + 0.21 \times e^{-t/t_{Co}}], \tag{7}$$

where A is a scaling constant that depends on the initial mass of ^{56}Ni, $t_{Ni} = 8.8$ d is the decay time of ^{56}Ni, and $t_{Co} = 111$ d is the decay time of ^{56}Co. For this work, we neglect the difference in the deposition functions of gamma-rays and positrons (Cappellaro et al. 1997), but comment on the separate effect of positrons below. Figure 1 gives simple model bolometric light curves with various degrees of gamma–ray leakage as determined by the timescale T_0.

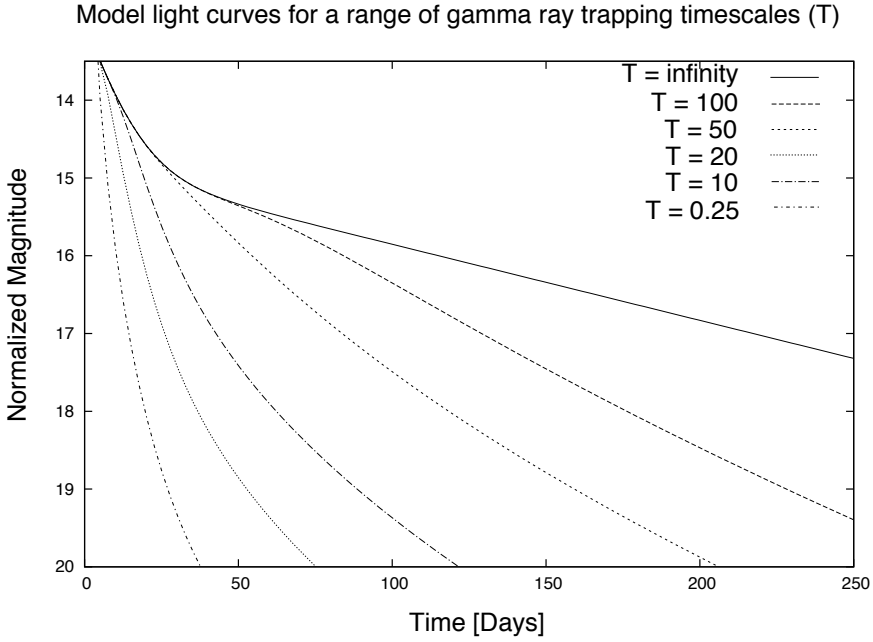

Fig. 1.— Model light curves for a range of the gamma-ray trapping timescale T_0 (arbitrary normalization). A trapping timescale of infinity corresponds to total trapping of gamma-rays from radioactive ^{56}Ni and ^{56}Co. In these figures, positrons are assumed to have the same effective opacity as gamma-rays.

3. Analysis

To estimate M_{ej}, E_{ke}, and T_0, we use data from the literature. Some of the supernovae that we discuss here have estimated UBVRI quasi–bolometric light curves, but not all. We have used the R–band as a proxy that allows us to treat most of the events in a somewhat homogeneous way, but also compare to bolometric data where it is available. For events with only R–band data, we neglect bolometric corrections and assume that the R–band light curves are proxies of the bolometric luminosity to within a constant scaling factor (See Lyman, Bersier & James 2014 for a discussion of estimating bolometric corrections for stripped–envelope supernovae). Figure 2 gives a comparison of the R–band and UVOIR light curves of three events, Type IIb SN 1993J, and two broad–lined SN Ic, SN 1998bw, and SN 2002ap, normalized at peak light. This figure shows that, for these events, the R–band is a reasonable representation of the quasi–bolometric light curve to times of hundreds of days. We have ignored reddening corrections for our R–band light curves, but such corrections have been made by the original authors who present the quasi–bolometric data. It seems unlikely that the results we present here are simply the result of variance in reddening, but this must be borne in mind. In some cases of sparse or absent R–band data, we employ V–band or other available data.

The sample for which there is good rise time data as well as long–time tail data is still sparse. The peak is used to estimate the rise time, t_r. For many of the more recent events and for some earlier nearby events, there is pre–maximum photometry. In the best cases, there are reasonably accurate estimates of the time of explosion (SN 1993J, Richmond et al. 1994; SN 2008D, Malesani et al. 2009, Modjaz et al. 2009). In other cases, the earliest data are up to two weeks prior to peak and thus are a good representation of the rise time (SN 1998bw, Patat et al. 2001; SN 1994I, Richman et al. 1996; SN 1999dn, Benetti et al. 2011; SN 2007Y, Stritzinger et al. 2009; SN 2007gr, Valenti et al. 2008a; SN 2009jf, Sahu et al. 2011; SN 2011bm, Valenti et al. 2012; SN 2011dh, Ergon et al. 2014, Marion et al. 2014). Note that even in these cases, the R–band peak may be delayed from the bolometric peak by several days. We have used the time to R–band peak in most cases, but recognize that some ambiguity is introduced in this way.

In yet other cases there is some pre–maximum data, but not as extensive as the previous cases. For cases where there is pre–maximum data more than a magnitude dimmer than maximum, we use the time from first observation to the peak in R–band as an estimate for the rise time. This is an underestimate by perhaps several days, or typically 10 – 20%. Examples are SN 1983N (FES data; Clocchiatti et al. 1997), SN 1996cb (Qui et al. 1999), SN 2002ap (Tomita et al. 2006), SN 2004aw (Taubenberger et al. 2006), and SN 2009bb (Pignata et al. 2011).

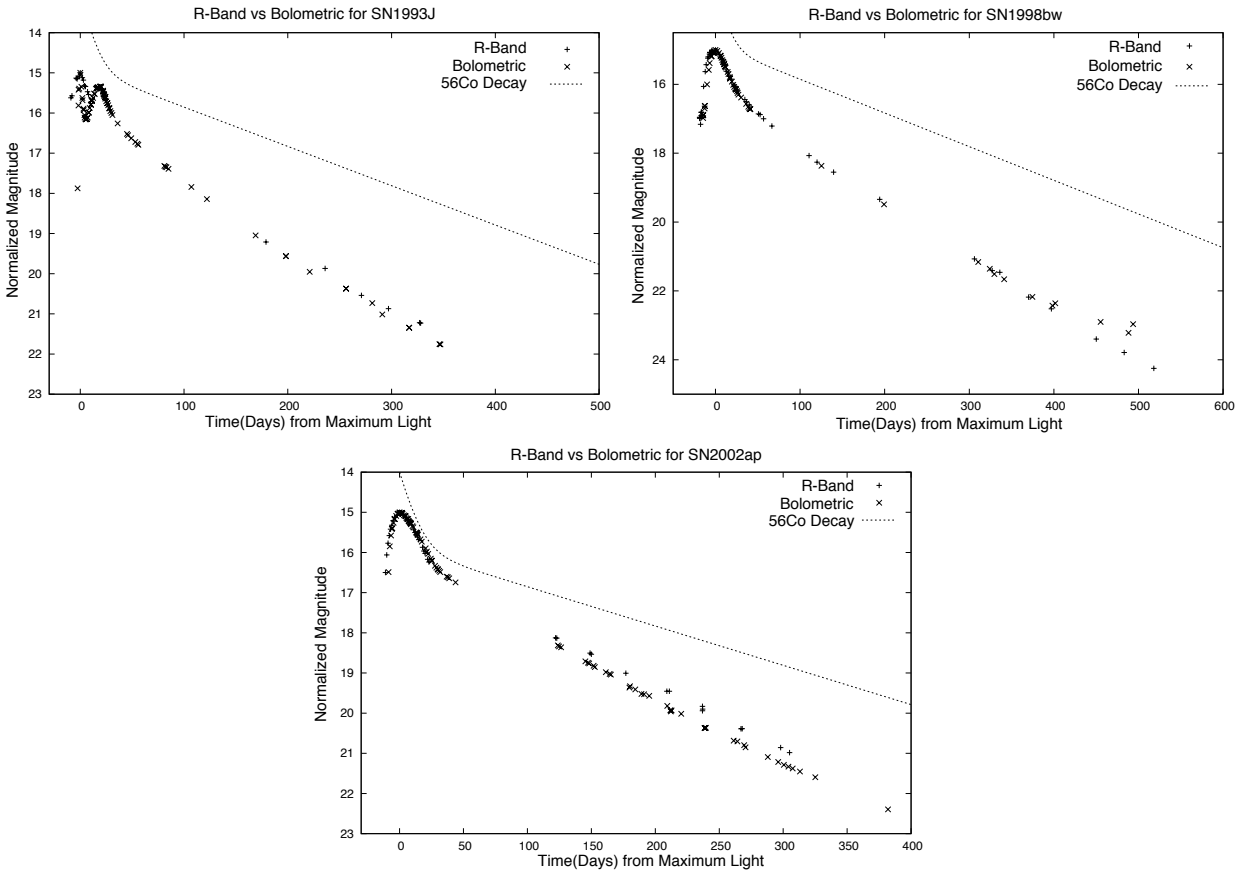

Fig. 2.— Comparison of R–band and quasi–bolometric light curves for three supernovae: SN 1993J (upper left panel); SN 1998bw (upper right panel); SN 2002ap (lower panel). Data are from Barbon et al. (1995); Richmond et al. (1994); Zhang et al. (2004) (SN 1983J); Patat et al. (2001); Clocchiatti et al. (2011) (SN 1998bw); and Tomita et al. (2006) (SN 2002ap).

In other cases, there is little or even no pre–maximum data. In these cases, we make estimates based on analogies to other events (SN 1983V, Clocchiatti et al. 1997; SN 1984L, Swartz & Wheeler 1991) or on the decline from maximum and estimate the time to decline by a magnitude from peak (SN 1990B, Clocchiatti et al. 2001). The light curves of the stripped–envelope events are typically asymmetric around the peak with more rapid rise than decline, so this post–maximum decline timescale almost surely overestimates the rise time. In these various cases, we have put our estimates in square brackets in Table 1 to highlight the uncertainty. The rise time comes in squared in the estimates of the mass and energy, so these estimates should be considered with caution.

Taddia et al. (2014) give a table containing observed R–band rise times. Most of these agree with our choices, but there are some discrepancies. We chose 17 d for the rise for

SN 1993J versus 22.53 d for Taddia et al. Our estimate is measured from the early minimum in the light curve, ignoring the initial fireball decline phase. We assume the subsequent rise is more representative of other events that were not caught so early and of the diffusion time we are attempting to constrain. We chose 15 d for SN 2007Y from Stritzinger et al. (2009), versus the 21 d assigned by Taddia et al. The latter seems to involve some extrapolation even beyond the early V–band data, but our value is surely a lower limit.

Estimates of velocity are taken from photospheric velocities given in the literature. For uniformity, we have tried to select whenever possible the velocity of the P Cygni absorption minimum of Fe II λ5169 measured at R–band maximum. While this line may be relatively free of blending, as may affect estimates based on Si II, there are still issues. In particular, the velocity measured in this way often declines rather rapidly from pre–maximum to post–maximum epochs. Velocities at bolometric maximum several days earlier would usually have been somewhat higher and there is the general concern as to whether any velocity measured in this way properly represents the scale velocity of the underlying model. Such considerations comes in especially sensitively in estimates of the energy. Cano (2013) and Lyman et al. (2014) also give compilations of photospheric velocities. In general, our estimates agree with theirs to within 20%. Exceptions are SN 2004aw where we determined 16,000 km s^{-1}, Cano gave 11,800 km s^{-1} and Lyman et al. give 11,000 km s^{-1}, and SN 2009bb, for which we determined 18,000 km s^{-1}, Cano gave 15,000 km s^{-1}, and Lyman et al. gave 17,000 km s^{-1}.

We use the late–time light curves to directly determine an estimate of T_0 and one standard deviation error bars by minimizing the χ^2 of the fit of Equation 6 to the data. To minimize the effect of scatter in the peak data, we only use the data after 50 d from maximum to determine the observed value of T_0. Table 1 also gives the measured values of T_0. The error given for SN 2007Y is especially, and probably artificially, low because there is sparse late–time data that is easy to fit.

For some objects in the sample here, Clocchiatti et al. (2008) also estimated values of T_0 from UBVRI quasi–bolometric light curves. Comparing the values derived here (first numbers, R–band; the numbers in parentheses are our estimate of the value based on quasi–bolometric data) with those given by Clocchiatti et al. (second numbers) we find: SN 1994I, 115 d vs 65 d; SN 1998bw, 192 (283) d vs 120 d; SN 2002ap, 186 (202) d vs 142 d; SN 1990B, 113 d vs 88 d. There are differences of 10 to 30% with our estimates somewhat on the high side. The difference is most likely due to our simple treatment that implicitly has the trapping of positrons decreasing in the same manner as for the gamma–rays. If positrons are trapped, as assumed by Clocchiatti et al., then for values of $T_0 \sim 100$ to 200d, the positron contribution will be comparable to that of the gamma–rays by 200 – 300 d. With this extra contribution to the luminosity, a light curve of given late–time slope can be accommodated

with a smaller value of the parameter T_0. In the first portion of our discussion comparing the observed decay time versus that predicted from the peak properties, as expressed in Equation 5, differences of $\lesssim 30\%$ are not significant since we are interested in discrepancies of factors of several. In §4 where we address the issue of estimating ejecta masses and energies from the tail, the decay time enters as the square and hence more sensitively. We address the issue of positron trapping again there.

Figures 3, 4, and 5 give the light curves we have compiled. For comparison purposes, the light curves have been shifted in time to a common peak and have been normalized to an arbitrary magnitude of 15.

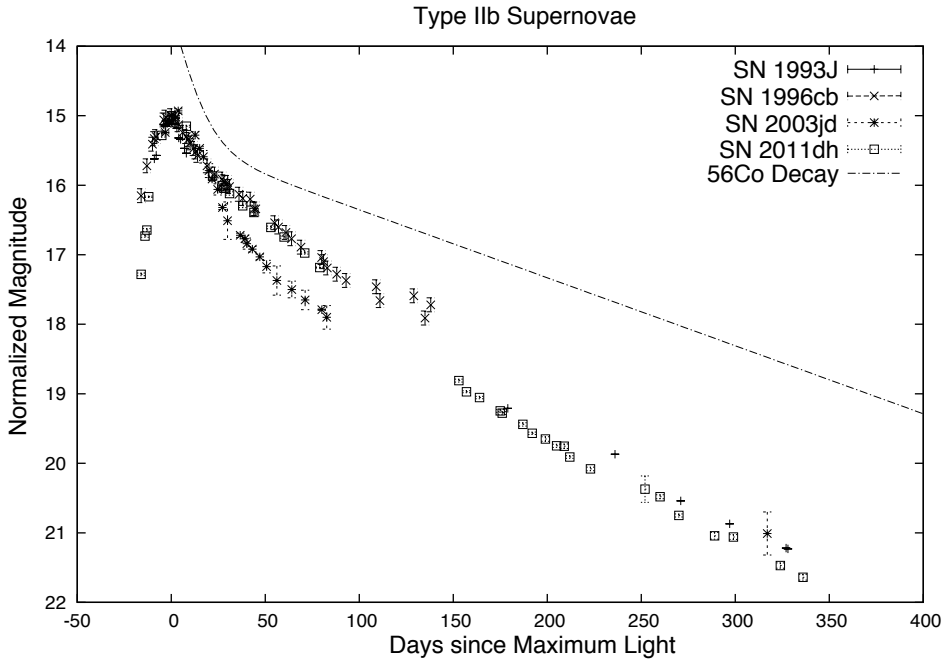

Fig. 3.— R–band light curves of a sample of SN IIb. Note the similar behavior around maximum and the very similar late–time light curves of SN 1993J and SN 2011dh for nearly 250 d, but the variation in the decline rate manifested by SN 1996cb (slower) and SN 2003jd (faster after peak, but comparable to SN 1993J later). The dot–dash line represents the total trapping of the energy of radioactive decay. Data are from Barbon et al. (1995); Richmond et al. (1994); Zhang et al. (2004) (SN 1993J); Qiu et al. (1999) (SN 1996cb); Valenti et al. (2008b) (SN 2003jd); Tsvetkov et al. (2012) (SN 2011dh; note that even later data is given in Ergon et al. 2015).

Figure 3 gives a sample of 4 SN IIb. They are all rather similar near peak, with similar rise times and early declines, but substantial departures from homogeneity set in beginning

about 30 d after maximum. The long–term light curves of these events are distinctly steeper than that given by full trapping of gamma-rays from ^{56}Co decay. There is a clear dispersion of the late–time decay times despite the similarity of the light curves near peak and the common spectral class. SN 1993J and SN 2011dh show very similar late–time light curves for nearly 350 d. SN 2003jd falls more steeply around 30 d after peak, but has a similar rate of decline at later times. SN 1996cb is slower at late time than the others. Its decay after 100 d is similar to that of total trapping, but a contribution from circumstellar interaction cannot be ruled out.

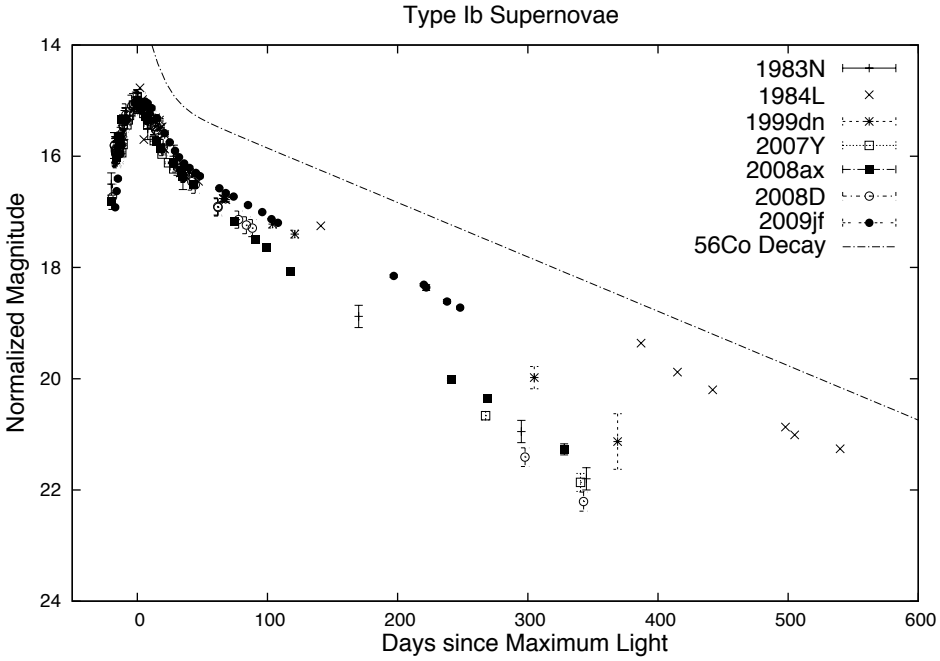

Fig. 4.— R–band light curves of a sample of SN Ib. Note the significant dispersion in the decline rate at late time. The dot–dash line represents the total trapping of the energy of radioactive decay. Data are from Clocchiatti et al. (1996) (SN 1983N); Swartz & Wheeler (1991) (SN 1984L); Benetti et al. (2011) (SN 1999dn); Stritzinger et al. (2009) (SN 2007Y); Malesani et al. (2009), Modjaz et al. (2009) (SN 2008D); Pastorello et al. (2008) (SN 2008ax); Sahu et al. (2011) (SN 2009jf).

Figure 4 gives a sample of 7 SN Ib. We have plotted V–band data for SN 1983N, r‘–band data for SN 2007Y, and bolometric data for SN 2008D and SN 2008ax. SN 2008ax is often classified as a SN IIb because some hydrogen was seen early on. By maximum, it looked like a classic SN Ib. We have classified it as a SN Ib here, but that particular choice does not affect our analysis in any substantial way. These seven events again are rather similar on the rise. SN 1984L flattens to be comparable to the radioactive decay slope, but SN 1984L

was a late–time radio emitter, so there might be some contribution to the light curve from collision with a circumstellar medium. SN 1999dn and SN 2009jf are similar on the tail for the first 100 d. SN 2009jf subsequently falls at a rate roughly comparable to cobalt decay until at least 250 d, but SN 1999dn falls more steeply at 300 to 400 d. SN 1983N, SN 2007Y, SN 2008D and SN 2008ax fall at very similar rates at late times, with SN 2008D being the steepest of this group.

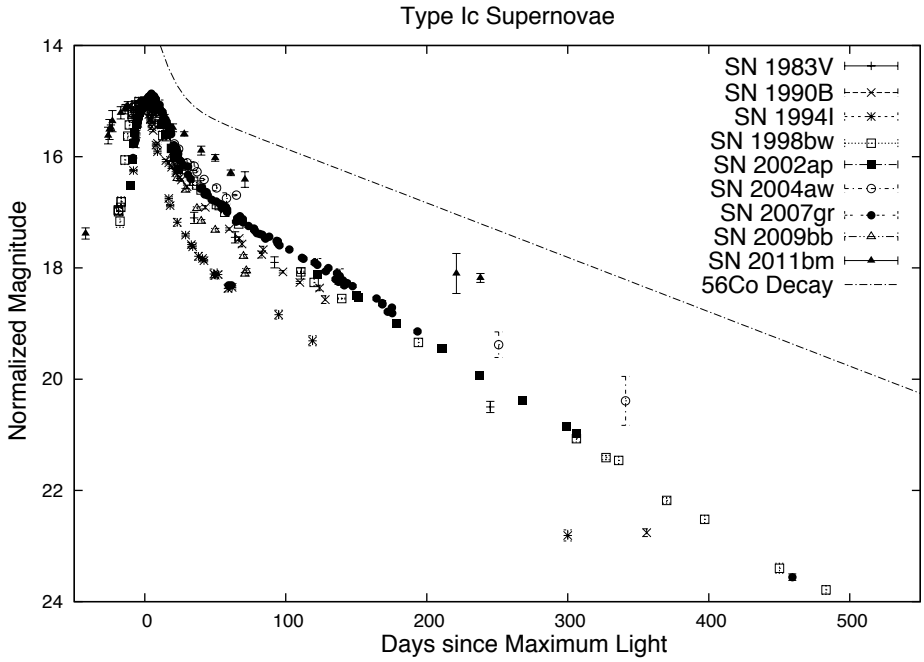

Fig. 5.— R–band light curves of a sample of SN Ic. The data for SN 1983V are V–band. Note the distinct rapid rise and decline of SN 1994I and the slower rise and decline of SN 2011bm. The post–peak decay of SN 2011bm closely follows the radioactive decay line. Otherwise, the relative homogeneity of the peaks leads to a large dispersion of late–time tails. The dot–dash line represents the total trapping of the energy of radioactive decay. Data are from Clocchiatti et al. (1997) (SN 1983V); Clocchiatti et al. (2001) (SN 1990B); Clocchiatti et al. (2008) (SN 1994I); Patat et al. (2001) (SN 1998bw); Tomita et al. (2006) (SN 2002ap); Taubenberger et al. (2006) (SN 2004aw); Pignata et al. (2011) (SN 2009bb); Valenti et al. (2012) (SN 2011bm).

Figure 5 gives a sample of 9 SN Ic. We have plotted B–band data for SN 1983V. There appears to be some true dispersion in the early peak widths. SN 2011bm has a distinctly wider peak. SN 1994I falls especially rapidly after maximum. SN 2009bb nearly rivals SN 1994I in terms of steepness of immediate post–maximum decline. There is clearly a large dispersion in the rate of decay of the late–time tails of the SN Ic. SN 2011bm continues to

decline slowly, with a late–time decay very comparable to that expected for ^{56}Co decay. The late–time light curves of the broad–line Type Ic SN 1998bw and SN 2002ap are very similar; SN 2004aw declines somewhat more slowly than the two broad–line events, and SN 1990B somewhat more rapidly. The light curve of SN 1994I flattens at very late times (300 d), which may have to do with partial trapping of positrons (Clocchiatti et al. 2008).

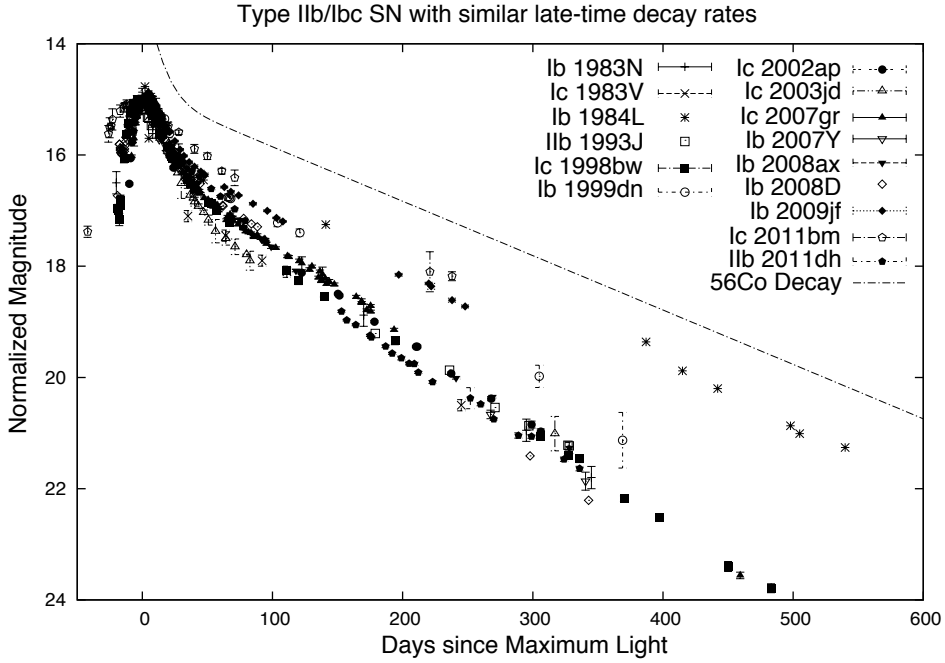

Fig. 6.— Light curves of a selected sample of SN IIb, Ib, and Ic with similar late–time decay rates. Note the relative homogeneity of the peaks and the bifurcation (in this small sample) of the late–time light curves into two groups. The slower–declining group has only SN Ib, but the more rapidly–declining group contains SN IIb, SN Ib and SN Ic, including high–velocity SN Ic. The dot–dash line represents the total trapping of the energy of radioactive decay. References to data are given in previous captions.

Figure 6 gives a selected sample of light curves that seem, by eye, to fall into two categories in terms of late–time tails. One group has a decline roughly comparable to ^{56}Co decay, and the other is significantly steeper. Among the first category with rather shallow late–time declines, Type Ib SN 1984L, Type Ic SN 2011bm, and perhaps Type Ib SN 2009jf are the only examples in our sample of late-time light curves that track ^{56}Co decay (corresponding to very large values of T_0). As remarked above, the late–time light curves of the Type Ib SN 1999dn and SN 2009jf are very similar up to 100 d, with SN 1999dn perhaps tracking ^{56}Co decay. Later data on SN 1999dn fall below this early common trend. Either SN 1999dn was not powered by ^{56}Co decay earlier, but perhaps by circumstellar interaction, or some

other effect, perhaps dust formation, arose after 200 d to suppress the optical light curve. In any case, most stripped–envelope supernovae decay considerably faster than expected for complete trapping of ^{56}Co.

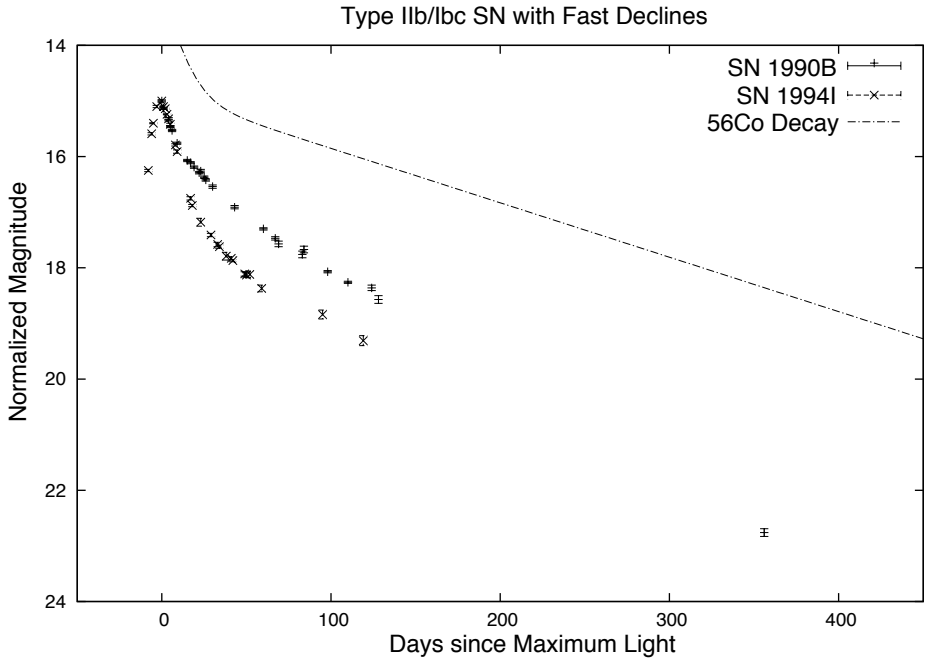

Fig. 7.— Light curves of two stripped–envelope supernovae with rather steep late–time decay rates, both SN Ic. The dot–dash line represents the total trapping of the energy of radioactive decay. References to data are given in previous captions.

The assortment of light curves of other SN IIb, SN Ib, and SN Ic, including some broad–line SN Ic, that fall in the second category in Figure 6 are also rather similar to one another, but with a distinctly different, steeper slope than those that might follow ^{56}Co decay. Interestingly, this group comprises 11 of our sample of 20 events. This group includes SN 1983V, but we note that the data are B–band, so the decline rate may be exaggerated. The light curves of SN 1983V in both V–band and B–band were very similar to those of SN 1993J in the respective bands (Clocchiatti et al. 1997), and the light curve we plot here is very similar to that of SN 1993J in R–band at late times, but it is appropriate to regard this comparison with some caution. There appears to be some dispersion in peak width for this particular subsample. Figure 7 presents data for two events that decay more rapidly at late times than most. Both are SN Ic. SN 1994I seems to fall more rapidly from peak than SN 1990B.

Figures 6 and 7 illustrate that neither spectral type nor similar peak light curves de-

termine the slope of the late–time tail, and that events of different spectral type can have remarkably similar late–time tails, as emphasized by Clocchiatti et al. (1996, 1997). The spectra and light curves of stripped–envelope supernovae near maximum light are not sufficient to fully classify them.

Table 1 gives for our sample of events, the observed values of v_{ph}, t_r, and T_0 and the value of T_0 estimated from Equation 5. We have also attempted to assign representative uncertainties to our estimates of v_{ph} and t_r. For v_{ph} we have assigned an uncertainty of 10%, or about $\pm$1000 km s^{-1} for the typical observed velocities. While not exact, this is a representative uncertainty. For t_r, we have also assigned an uncertainty of 10% for many of the events, 2 or 3 d for typical events, but an uncertainty of 20% for the events where, for various reasons, the rise time is especially ill–determined. The values of t_r for these events are given in square brackets in Table 1 to draw attention to these events. We have then propagated these uncertainties through the estimate of T_0 from Equation 5 and for other quantities to be discussed in §4. We have assumed for this exercise that the observed values of v_{ph}, t_r, and T_0 are uncorrelated, but this may not be completely true. The predicted value of T_0 in Equation 5 only depends linearly on the rise time and on the square root of the velocity. Uncertainty in these parameters are relatively unimportant to that particular quantity. The effects in which we are interested are typically factors of several in T_0, as illustrated in Table 1.

For illustration, we have also made an analytic fit to the tail for the group of 11 events that form a nearly common locus in Figure 6. Restricting the analysis to more than 50 d from maximum, we can neglect the contribution of the $e^{-t/t_{Ni}}$ term in Equation (7). Anticipating that T_0 is fairly large, then at 50 d the term $e^{-(T_0/t)^2}$ in Equation (6) is essentially zero and can also be neglected. Making those two assumptions, one can write the magnitude $M = -2.5logL + K$ at the two epochs, 50 d and 400 d, where the similar track in Figure 6 passes through about magnitude 17 and 22.5, respectively. Using these values, the resulting parameter is $T_0 = 158$ d, corresponding to ~ 0.016 mag d^{-1}, a reasonable estimate to the range of values for these 11 events presented more formally in Table 1.

Figure 8 shows the observed value of T_0 versus that estimated from the peak properties using Equation 5. This exercise shows clearly that the values of v_{ph} and t_r, and hence the values of M_{ej} and E_{ke}, derived from the peak behavior are poor predictors of the late–time behavior. The discrepancies are not subtle. The directly measured values of T_0 occasionally agree within a factor of two of those estimated from the peak properties, but the discrepancies are routinely factors of 2 to 4, and can be as much as a factor of 10(SN 1984L). In no case is the estimate of T_0 from the peak properties greater than that determined from direct observations of the late–time tail.

Table 1. Estimated vs. Observed Timescale of Late–Time Decay of Stripped–Envelope Supernovae

Event SN	Type	v_{ph} $10^9 cms^{-1}$	t_{rise} d	T_0 Est.(d)	T_0 Obs.(d)	Band
1983N	Ib	0.78 ± 0.08	$[16 \pm 3]^*$	58 ± 12	166 ± 16	V
1983V	Ic	1.4 ± 0.14	$[20 \pm 4]^*$	54 ± 11	151 ± 7	B
1984L	Ib	1.0 ± 0.1	$[20 \pm 4]^*$	64 ± 13	660 ± 109	V
1990B	Ic	1.1 ± 0.1	$[20 \pm 4]^*$	61 ± 13	113 ± 5	R
1993J	IIb	0.75 ± 0.08	17 ± 1.7	63 ± 7	135 ± 5	Bol
1994I	Ic	1.15 ± 0.12	9 ± 0.9	27 ± 3	115 ± 6	R
1996cb	IIb	0.9 ± 0.1	25 ± 2.5	85 ± 10	152 ± 15	R
1998bw	Ic	1.4 ± 0.14	14.4 ± 1.4	39 ± 4	192 ± 6	R
1999dn	Ib	1.0 ± 0.1	$[15 \pm 3]^*$	48 ± 10	220 ± 14	R
2002ap	Ic	1.5 ± 0.15	$[9 \pm 0.18]^*$	24 ± 5	186 ± 8	Bol
2003jd	IIb	1.4 ± 0.14	$[20 \pm 4]^*$	54 ± 11	237 ± 81	R
2004aw	Ic	1.6 ± 0.16	$[35 \pm 7]^*$	89 ± 18	206 ± 123	R
2007Y	Ib	0.9 ± 0.09	15 ± 1.5	51 ± 6	114 ± 1	r'
2007gr	Ic	0.64 ± 0.06	15 ± 1.5	60 ± 7	157 ± 4	R
2008D	Ib	1.0 ± 0.1	20 ± 2	64 ± 7	107 ± 3	R
2008ax	Ib	0.8 ± 0.08	22 ± 2.2	79 ± 9	175 ± 11	Bol
2009bb	Ic	1.8 ± 0.18	$[9 \pm 1.8]^*$	22 ± 4	57 ± 20	R
2009jf	Ib	1.0 ± 0.1	25 ± 2.5	80 ± 9	315 ± 24	R
2011bm	Ic	0.75 ± 0.08	45 ± 4.5	170 ± 19	308 ± 41	R
2011dh	IIb	0.69 ± 0.07	22 ± 2.2	85 ± 10	210 ± 10	R

*Entries in square brackets are especially uncertain; see text

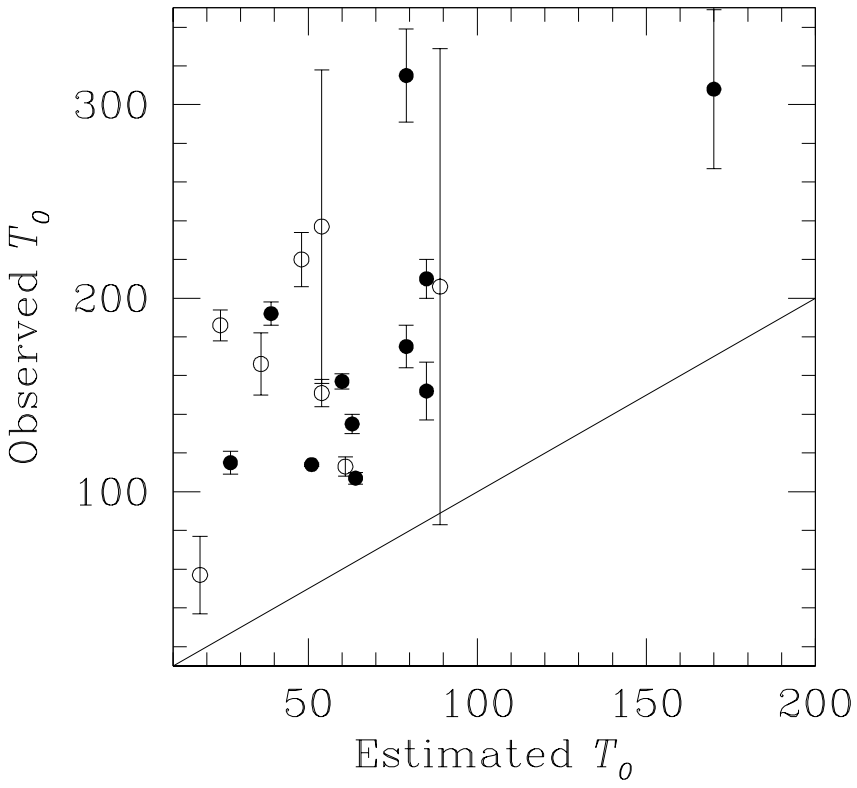

Fig. 8.— The values of the timescale, T_0, obtained from fits to the late–time data (with 1–σ error bars) are plotted against the values of T_0 predicted from the properties of the peak according to Equation 5. The diagonal line represents equality of the two time scales. The observed values are considerably higher than the predicted values, indicating a significantly slower late–time decay than predicted. Open symbols represent events for which the rise time is especially uncertain (square brackets in Table 1). Data for SN 1984L have been omitted as they are off the scale of the plot.

4. Discussion

This analysis defines four dilemmas associated with the late–time light curves of stripped–envelope supernovae. (1) The relatively similar peak properties often belie a considerable spread in the properties of the late–time tail. (2) Even for events with similar peaks and tails, the properties derived from the peak seem to be incommensurate with the behavior of the tail. (3) Events with different spectral types can, nevertheless, have rather similar late–time decay. (4) Both typical SN Ic and broad–lined SN Ic can have similar late–time decay despite the nominal significant differences in energy associated with the broad lines of the latter.

To elucidate these various, related, dilemmas, we can write expressions for the ejected mass and energy in terms of the observed properties as follows. From the peak, we have from Equations 1 and 3

$$M_{ej} = \frac{1}{2}\frac{\beta c}{\kappa} v_{ph} t_r^2, \tag{8}$$

and

$$E_{ke} = \frac{3}{20}\frac{\beta c}{\kappa} v_{ph}^3 t_r^2, \tag{9}$$

and from the tail we have from Equation 4, invoking $E_{ke} = \frac{3}{10} M_{ej} v_{ph}^2$,

$$M_{ej} = \frac{3}{10}\frac{v_{ph}^2 T_0^2}{C\kappa_\gamma}, \tag{10}$$

and

$$E_{ke} = \left(\frac{3}{10}\right)^2 \frac{v_{ph}^4 T_0^2}{C\kappa_\gamma}. \tag{11}$$

The complex relationships among the early and late photometric behaviors of different spectral types of stripped–envelope supernovae can be illustrated by comparing light curves of several well–observed events that have data in Table 1. The two Type Ib SN 1994L and SN 2008D have very similar rise times and photospheric velocities, yet very different late–time tails, illustrating point (1). The typical Type IIb event SN 2011dh and the hydrogen–contaminated Type Ib event SN 2008ax had similar rise times and photometric velocities of $\sim$ 22 d and $\sim 8,000$ km s^{-1}, respectively. For similar opacities, one might expect similar ejecta masses and energies and thus similar tails. The tails were similar, but also similar to that of Type Ic SN 2007gr, a congruence that defies easy explanation, point (3) above.

Furthermore, not all events with similar tails have similar peak properties. SN 2007gr had a somewhat more rapid rise, $\sim$ 15 d, and lower photospheric velocity near peak, $\sim$ 6400 km s^{-1}. Both of these differences suggest that, for similar opacities, the ejecta mass

($\propto v_{ph} t_r^2$; Equation 8) and the kinetic energy ($\propto v_{ph}^3 t_r^2$; Equation 9) should be less than for SN 2011dh and SN 2008ax. The fact that the late–time tail of SN 2007gr is similar to those of SN 2011dh and SN 2008ax and others of different spectral class would then seem to require an unexpected correlation of the ejecta mass and energy. The broad–line Type Ic SN 2002ap had a rise time of ~ 10 d and a photospheric velocity of $\sim 15,000$ km s^{-1}. Based on the peak properties, and again assuming similar opacities, SN 2002ap should have about the same ejecta mass as SN 2007gr, but a kinetic energy that is larger by about a factor of 4. It is difficult in this simple framework to understand how their late–time tails are similar, illustrating point (4).

Equations 10 and 11 show that the constraint of similar late–time light curves, those with similar values of T_0, implies that $M_{ej} \propto v_{ph}^2$ and $E \propto M_{ej}^2 \propto v_{ph}^4$. With these relations, the similar tails imply that the ejecta mass of SN 2002ap must be larger than that of SN 2011dh and SN 2008ax by a factor of ~ 4 and the energy larger by a factor of ~ 16 while maintaining similar late–time decay.

Even for individual events with similar peak and tail properties, it is difficult to reconcile the two phases, point (2) above. The constraints from the width of the peak, $M_{ej} \propto v$ and $E \propto v^3$ for a constant opacity and given light curve rise time, are different from those associated with the slope of the tail, $M_{ej} \propto v^2$ and $E \propto v^4$ for a given γ-ray opacity and late–time decay time. A particular supernova can only have one M_{ej} and one E, so both of these sets of constraints need to be at least approximately satisfied. Since the peak relations predict $E \propto M_{ej}^3$ and the tail relations predict $E \propto M_{ej}^2$, there is a conflict. Poznanski (2013) makes an empirical case that the energy scales as the cube of the progenitor mass for SN IIP, but no current core–collapse simulations predict $E \propto M_{ej}^2$ or $E \propto M_{ej}^3$.

The resolution of this peak/tail conflict may involve consideration of the mean UVOIR opacity near the peak, κ. We note from Equations 8 and 9 that the observed parameters do not constrain the ejected mass and energy but only the degenerate combinations κM_{ej} and κE_{ke}. By invoking the constraint that the ejected mass determined from peak parameters be equal to the ejected mass constrained from tail parameters, the mean opacity can be formally expressed in terms of constants (β and C depend slightly on density structure), the reasonably well–known value of κ_γ, and of the observed rise time, photospheric velocity near peak, and the decay time as

$$\kappa = \frac{5}{3} \beta c C \frac{\kappa_\gamma}{v_{ph}} \left(\frac{t_r}{T_0} \right)^2 . \tag{12}$$

For typical parameters this can be expressed as

$$\kappa = 0.01 \text{ cm}^2 \text{ g}^{-1} \frac{(\kappa_\gamma / 0.03 \text{cm}^2 \text{ g}^{-1})}{v_{ph,9}} \left(\frac{t_{r,10}}{T_{0,100}} \right)^2 . \tag{13}$$

where $t_{r,10}$ is the rise time in units of 10d and $T_{0,100}$ is the tail decay time in units of 100d. We emphasize that this expression for the opacity is basically determined by the observed parameters, v_{ph}, t_r, and T_0.

Equations 8, 9, 10, and 11 suggest other interesting relations. For a given ejected mass and energy, there is a degeneracy between κ and the rise time, t_r, such that one can write

$$\frac{\kappa}{t_r^2} = \left(\frac{5}{6}\right)^{1/2} \beta c \left(\frac{C\kappa_\gamma E_{ke}}{T_0^2}\right)^{1/4} M_{ej}^{-1}. \tag{14}$$

For events with similar rise times and decay times, this implies that $\kappa \propto E_{ke}^{1/4} M_{ej}^{-1}$.

Using Equations 10 and 11, one can also write

$$v_{ph} = \left(\frac{10}{3} C\kappa_\gamma M_{ej}\right)^{1/2} T_0^{-1}, \tag{15}$$

and

$$v_{ph} = \left(\frac{10}{3}\right)^{1/2} (C\kappa_\gamma E_{ke})^{1/4} T_0^{-1/2}, \tag{16}$$

giving the photospheric velocity (mean ejecta velocity) as functions of the ejected mass and energy. We note that Equations 15 and 16 are degenerate in the quantities $\kappa_\gamma M_{ej}$ and $\kappa_\gamma E_{ke}$. We have assumed that κ_γ is less dependent on explosion parameters than κ, but have kept the κ_γ dependence explicit to remind of that dependence.

Note added in proof: *A small, but significant variation in the arguments we present here would be to consider the mass given by Equation 8 to not represent* $M_{\rm ej}$*, but the quantity* $M_{\rm diff}$*, the mass involved in diffusion for which the opacity* $\kappa \sim 0.1$ *cm*^{2} *g*$^{-1}$ *is relevant. From this perspective, the LHS of Equations 12 and 13 would become* $\kappa(M_{\rm diff}/M_{\rm ej})$ *and hence*

$$\frac{M_{diff}}{M_{ej}} = \frac{5}{3} \beta c C \frac{\kappa_\gamma}{\kappa v_{ph}} \left(\frac{t_r}{T_0}\right)^2, \tag{17}$$

or

$$\frac{M_{diff}}{M_{ej}} = 0.1 \text{ cm}^2 \text{ g}^{-1} \frac{(\kappa_\gamma/0.03\text{cm}^2 \text{ g}^{-1})}{(\kappa/0.1\text{cm}^2 \text{ g}^{-1}) v_{ph,9}} \left(\frac{t_{r,10}}{T_{0,100}}\right)^2. \tag{18}$$

For $\kappa \sim 0.1$ *cm*^{2} *g*$^{-1}$*, Equation 18 would then give* $M_{\rm diff}/M_{\rm ej} \sim 0.1$ *for fiducial parameters, strongly suggesting that only a rather small portion of the ejecta is ionized. With this redefinition of the mass from Equation 8, corresponding changes should be made in Equations 5, 14, 15, and 16.*

The mean opacity derived in this way tends to be ~ 0.01 cm^2 g^{-1} for events with typical peak properties and a late–time decline of $T_0 \sim 160$ d or ~ 0.016 mag d^{-1} that characterizes

the various stripped–envelope events considered in the examples above; this is considerably smaller than the estimates normally applied in this context, $\kappa \sim 0.1$ cm^2 g^{-1}. We note that the two–component model fit of Vinkó et al. (2004) to SN 2002ap required a mean opacity of order 0.01 cm^2 g^{-1} to fit the observed evolution of the photospheric velocity. If this analysis, constrained by the decay properties of the tail, is reasonably correct, then the effective opacity that determines the peak properties may be quite low. Many estimates of the ejected mass and energy in the literature that assume or compute a higher opacity could be too low by as much as a factor of 10.

This analysis shows that the mean opacity that dictates the peak properties of stripped-envelope supernovae may have been over–estimated in many cases. If so, this would help to resolve dilemma (2) outlined above and suggest that results derived from the peak alone may be suspect. This analysis has not resolved the other dilemmas, but suggests some new perspectives to bring to the study of stripped–envelope and perhaps other core–collapse supernovae, suggesting correlations between the energy and ejected mass required to account for the tail behavior and how the opacity and expansion velocity might depend on the ejected mass and energy.

We summarize the implications of these considerations for the supernova sample we analyze here in Table 2. Columns 3 and 4 give the estimates of the ejected mass and energy derived from peak properties, scaled to a value of the mean opacity of 0.1 cm^2 g^{-1}, from Equations 8 and 9. Columns 5, 6, and 7 give the ejected mass and energy according to Equations 10 and 11 and the opacity according to Equation 12 that would be required to yield the latter values of mass and energy. We have propagated the uncertainties in the observed parameters v_{ph}, t_r, and T_0 to express the uncertainties in the various derived quantities. As noted in §3, we formally assume that the uncertainties in these observed quantities are uncorrelated. Equations 14, 15, and 16, for instance, suggest that this may not be true. We reserve a deeper study of this issue for future work.

As also noted in §3, our previous determinations of the late–time decay parameter, T_0, are probably overestimates because we treated the leakage of positrons as similar to that of gamma–rays. While positrons may not be completely trapped, there is evidence that they are at least partially so in SN 1994I (Clocchiatti et al. 2008). The uncertainty in the positron deposition function therefore leads to an intrinsic uncertainty in the quantitative value of T_0 that comes in squared in Equations 10 and 11. Assuming that positrons are completely trapped would lead to an underestimate of T_0 if they are only partially trapped.

We have accounted for the uncertainty in positron trapping and other uncertainties in the following way in Table 2. For events for which our uncertainties in the observed value of

Table 2. Estimates of Ejecta Mass, Energy, and Mean Optical Opacity

Event SN	Type	$\left(\frac{\kappa}{0.1\ \mathrm{cm^2 g^{-1}}}\right) M_{ej}$ [1] $M_\odot$	$\left(\frac{\kappa}{0.1\ \mathrm{cm^2 g^{-1}}}\right) E_{ke}$ [2] 10^{51} erg	M_{ej} [3] $M_\odot$	E_{ke} [4] 10^{51} erg	κ [5] cm^2 g^{-1}
1983N	Ib	1.5 ± 0.5	0.56 ± 0.2	$< [13 \pm 6]^*$	$< [4.6 \pm 2]^*$	$> [0.012 \pm 0.007]^*$
1983V	Ic	4.4 ± 1.3	5.1 ± 1.7	$< [34 \pm 11]^*$	$< [39 \pm 14]^*$	$> [0.013 \pm 0.006]^*$
1984L	Ib	3.1 ± 0.9	1.9 ± 0.6	$< [330 \pm 190]^*$	$< [200 \pm 120]^*$	$> [0.0010 \pm 0.0006]^*$
1990B	Ic	3.4 ± 1	2.5 ± 0.8	12 ± 4	5.1	0.047
1993J	IIb	1.7 ± 0.3	0.57 ± 0.1	$< 7.7 \pm 2.4$	$< 2.6 \pm 0.9$	$> 0.022 \pm 0.007$
1994I	Ic	0.72 ± 0.13	0.57 ± 0.1	4.2	3.3	0.017
1996cb	IIb	4.4 ± 0.8	2.1 ± 0.5	$< 14 \pm 7$	$< 6.8 \pm 3$	$> 0.031 \pm 0.015$
1998bw	Ic	2.3 ± 0.4	2.6 ± 0.6	21	25	0.010
1999dn	Ib	1.7 ± 0.5	1.0 ± 0.3	$< 36 \pm 14$	$< 22 \pm 9$	$> 0.0048 \pm 0.002$
2002ap	Ic	0.94 ± 0.3	1.3 ± 0.4	34	47	0.0027
2003jd	IIb	4.7 ± 1.4	6.3 ± 2	$< [95 \pm 80]^*$	$< [127 \pm 110]^*$	$> [0.0049 \pm 0.004]^*$
2004aw	Ic	15 ± 5	23 ± 8	$< [82 \pm 90]^*$	$< [125 \pm 140]^*$	$> [0.019 \pm 0.02]^*$
2007Y	Ib	1.6 ± 0.3	0.76 ± 0.2	$< 7.9 \pm 1.5$	$< 3.8 \pm 0.9$	$> 0.020 \pm 0.004$
2007gr	Ic	1.1 ± 0.2	0.27 ± 0.06	$< 7.6 \pm 2$	$< 1.9 \pm 0.6$	$> 0.015 \pm 0.004$
2008D	Ib	3.1 ± 0.5	1.9 ± 0.4	$< 8.6 \pm 2$	$< 5.1 \pm 1.6$	$> 0.036 \pm 0.01$
2008ax	Ib	3.0 ± 0.5	1.1 ± 0.3	$< 15 \pm 6$	$< 5.6 \pm 2.3$	$> 0.020 \pm 0.008$
2009bb	Ic	1.1 ± 0.3	2.2 ± 0.7	$< [7.9 \pm 7]^*$	$< [15 \pm 13]^*$	$> [0.014 \pm 0.013]^*$
2009jf	Ib	4.9 ± 0.8	2.9 ± 0.6	$< 74 \pm 30$	$< 44 \pm 19$	$> 0.0065 \pm 0.003$
2011bm	Ic	12 ± 2	4.0 ± 0.9	$< 40 \pm 21$	$< 13 \pm 7$	$> 0.029 \pm 0.016$
2011dh	IIb	2.6 ± 0.4	0.74 ± 0.16	$< 16 \pm 5$	$< 4.5 \pm 1.6$	$> 0.016 \pm 0.006$

*Entries in square brackets are especially uncertain; see text

[1]Equation 8; [2]Equation 9; [3]Equation 10; [4]Equation 11; [5]Equation 13

T_0 were large (SN 1984L, SN 2003jd, SN 2004aw, SN 2009bb) we take the results for ejected mass, energy, and mean opacity based on the slope of the tail to be essentially undetermined, but present the values formally derived in square brackets. We also regard events without decent R–band or quasi–bolometric light curves (SN 1983N, SN 1983V, SN 1984L) to be ill–undetermined in this context and also present the associated data in square brackets. For events for which we have determined a late–time decay here with an exaggerated treatment of positron leakage, the majority of the events, we take the results to be upper limits on ejecta mass and energy and a lower limit on the mean opacity. Finally, for the few events for which Clocchiatti et al. (2008) estimated T_0 assuming complete trapping (SN 1994I, SN 1998bw, SN 2002ap, SN 1990b), we give estimates based on those values of T_0 (65d, 120d, 142d, and 88d, respectively), recognizing that these could be lower limits on the ejecta mass and energy and upper limits on the mean opacity. Clocchiatti et al. do not give uncertainties for their values of T_0 so we have not assigned formal uncertainties for these four events. From the uncertainties in v_{ph} and t_r alone, there would be uncertainties in the derived quantities of the order of 10 to 20%.

The limits we derive for SN 1984L are quite extreme, as follows from the large value of $T_0 \sim 660$d we find to fit the flat tail. As the ejecta mass increases, it should become more difficult to determine a precise value of T_0. The standard deviation we find, 109 d, is substantial but still rather small compared to the best–fitting value. At the 3σ lower limit on T_0, the estimates would be less by about a factor of 4, but still large. We may have underestimated the uncertainty here. In any case, the propagated uncertainties from all the observed values make the estimates for SN 1984L from the tail properties indeterminate. As noted above, the large uncertainties on SN 2003jd, SN 2004aw, and SN 2009bb mean that the formal results for them are also of little import. For the other events with upper limits to the ejecta mass and energy in Table 2, there is a suggestion of considerable spread in derived values.

Of special interest are the results for the events where the observed values of T_0 were determined in the context of a model that included positron trapping. For SN 1990B, the results for the ejecta mass and energy were of order a factor of 2 larger using the tail properties rather than the peak properties with the chosen mean opacity. For SN 1994I, the discrepancy was even larger, about a factor of 5. The cases of greatest interest were the broad–lined events, SN 1998bw and SN 2002ap, where the discrepancy in prediction is an order of magnitude or more.

5. Conclusions

This analysis has enunciated four dilemmas associated with the late–time light curves of stripped–envelope supernovae. (1) There is more heterogeneity in the tail properties than suggested by analyses of the peak alone. (2) The properties derived from the peak are often inconsistent with the properties of the tail. (3) Events with different spectral types can have rather similar tails. (4) Both typical SN Ic and broad–lined SN Ic can have similar late–time decay despite the implied differences in energy.

The values for ejecta mass and energy derived from the peak and the parameters that determine them frequently predict too steep a late–time decline, especially in simple models that assume a constant opacity over the peak of ~ 0.1 cm^2 g^{-1}. The physics of the late–time light curves is fairly simple, so the discrepancies may lie in the physics of the peak, despite the similarity of the immediate post–peak decline determined by Drout et al. (2011), Cano (2103), Lyman et al. (2014) and Taddia et al. (2015). Care must be taken with values of the ejecta mass and kinetic energy derived with simple estimates based only on the properties of the peak.

Our primary goal was not to derive ejecta masses and kinetic energies, rather to caution that these quantities can be sensitive to the way the data are selected and employed. Nevertheless, we can compare these quantities with related work. We note that Drout et al. (2011) employed a measure of the rate of decline to determine estimates of masses and energies, but that this time was in some instances shorter than the observed portion of the rise. The rise times we present in Table 1 are typically a factor of 2 – 3 larger than those given for the same events by Drout et al. Drout et al. also assigned v_{ph} in only two bins, 10,000 km s^{-1} for SN Ib and normal SN Ic and 20,000 km s^{-1} for SN Ic-BL. This will tend to mute the true dispersion of the physical properties of the supernovae that are related to differences in observed velocity. Also in contrast, Cano (2013) gives mean values for v_{ph} for SN Ib of 8027 km s^{-1}, for SN Ic of 8470 km s^{-1}, and for SN Ic-BL of 15,114 km s^{-1}. Cano does not discriminate between v_{ph} and $< v >$ as we have here. For our constant–opacity peak models with $\kappa = 0.1$ cm^2 g^{-1}, we tend to assign lower values of M_{ej} and E_{ke} than does Cano (for SN 1983N, SN 1999dn, SN 2002ap, SN 2007gr, SN 2008D, SN 2009jf, and SN 2011bm), but agree rather closely in several cases (SN 1994I, SN 2003jd, SN 2007Y, and SN 2009bb). We assign higher values than Cano for SN 2004aw. We cannot compare directly to Taddia et al. (2015) because their sample was based on SDSS objects not discussed in the general literature. The fits of Taddia et al. were mostly for light curves of less than 60 d after maximum. Their fitting procedure also involved a construction that employed more parameters than do ours. In a sense, the ratio of our values, $T_{0,obs}/T_{0,est}$, is another parameter determined by our process. Lyman et al. (2014) also use a measure of the decline

rate, rather than the rise, to determine the characteristic light curve "width" and employ a two–parameter fitting procedure similar to that of Taddia et al. to fit light curve properties up to about 80 d after maximum.

The analysis of the light curves of stripped–envelope supernovae has a long history. Ensman & Woosley (1988) invoked clumping as a possible way to address the difficulty of reproducing the peak/tail contrast. Clocchiatti & Wheeler (1997) discussed the possibility that the dynamics were in some fashion "non–homologous" with part of the ejecta remaining in a dense core. Maeda et al. (2003) constructed a two–component model that could fit the data better by dint of having extra parameters. They ascribed the second component to a dense inner region, analogous to the "non–homologous" component of Clocchiatti & Wheeler, to asymmetries in the explosion. Subsequent work has also invoked simple models with more parameters and hence more elaborate fits (Cano et al. 2014; Lyman et al. 2014; Taddia et al. 2015). The enduring problem has been to get the physics of the peak to agree with the physics of the tail. Most suggested solutions have focused on the processes of gamma–ray deposition. Here we suggest that the treatment of the opacity may be critical. In truth, the two are intimately related and must be treated together and self-consistently.

A possible factor that could yield a narrower peak for a given ejecta mass and kinetic energy and account for the low mean opacity suggested by Equation 13 is recombination that would give a time–dependent discontinuity in the opacity, akin to that in hydrogen in SN IIP. Ensman & Woosley (1988) made the first detailed quantitative models of SN Ib light curves based on helium cores from massive stellar models. They also presented one of the few careful exegeses of the nature of recombination fronts and their effect on opacity in this context. Whereas many simple models invoke a constant mean opacity over the peak of stripped–envelope models, the opacity is very sensitive to temperature, density, and expansion effects (Höflich, Müller & Khokhlov 1993; Pinto & Eastman 2000). Interestingly, the models of Ensman & Woosley produced less peak–to–tail contrast than the observations, rather than giving too steep a tail decline, the problem we have focused on here. In hindsight, this is because Ensman & Woosely employed rather massive helium–star models that retained a substantial fraction of the ejecta mass as helium. In their models, all the helium and much of the oxygen recombined before maximum, yielding a significant mass that had low opacity and contributed little to the optical diffusion time. Most of the opacity over the peak was contributed by the relatively low mass of the inner iron and silicon layers. The low effective opacity (Ensman & Woosley mention a typical value of 0.003 cm^2 g^{-1}) allowed them to fit the peak of SN 1983N with a rather large ejecta mass, but the whole ejecta mass contributed to the subsequent gamma-ray trapping, hence yielding excessively flat late–time light curves.

Subsequently, models of stripped–envelope light curves have invoked smaller ejecta

masses. Detailed hydrodynamic models that have included complex prescriptions for the opacity have yielded rather large mean opacities, ~ 0.1 cm^2 g^{-1}. This class of models nearly always found the late–time light curve to decline too steeply. Attempts to correct this problem have often addressed adjustments to the structure that would affect the gamma–ray trapping. The issue then arises as to whether these models that faded too quickly on the tail had, by assumption or computation, too large an effective opacity over the peak and hence too small an ejecta mass and too small an effective gamma–ray optical depth.

The UVOIR opacity that governs the shape of the peak is intrinsically complex with dependence on density, temperature, and composition and on nonLTE, nonthermal and expansion effects. Recombination depends on adiabatic expansion and cooling; subsequent reionization and increase in the opacity depends on the deposition of energy from radioactive decay. Recombination can lead to a situation where the opacity is a sensitive function of both space and time with the net effect being to decrease the effective opacity and thus yield a narrower peak light curve for a given ejecta mass. The models of Ensman & Woosley (1988) amply illustrate that there can be significant recombination effects on the mean effective opacity even in spherically–symmetric models. In the context of SN 1994I, Kleiser & Kasen (2014) also noted that the recombination of oxygen could lead yield a narrower peak (see also Piro & Morozova (2014). Some numerical models in the literature set a floor on the opacity. It is possible that this floor is set too high.

This raises the issue of how much cold, neutral material may exist in the ejecta of various types of stripped–envelope supernovae near peak. There must be some excited He I in both SN IIb and SN Ib. What is less clear is whether or not there may be a substantial amount of helium that is not excited by gamma-ray deposition. Dessart et al. (2012) argue that even with an appreciable layer of helium, a supernova would not appear as a SN Ib without outward mixing of ^{56}Ni. In principle, there could be a considerable amount of unexcited helium even in SN Ic. In each spectral type, and especially for SN Ic, the presence of a significant mass of cold, neutral helium will also affect the spectrum. A distinct identifying feature of SN Ic is the strong absorption corresponding to [O I] λ7774. This is one of the strongest features in the spectra of SN Ic, being distinctly stronger than in SN Ib (Matheson 2001). Models that include a significant mass of unexcited helium decelerate the oxygen and hence tend to produce oxygen lines that are too shallow, red, and narrow to correspond to the observed feature in typical SN Ic (Dessart et al. 2012).

Asymmetries in the explosions of stripped–envelope supernovae almost surely play a significant role. From spectropolarimetry, we know that stripped–envelope supernovae are asymmetric and that different elements are ejected at different angles (Maund et al. 2009). It is instructive to contemplate the image of the SN IIb Cas A, rent by jets and riddled with

irregularities due to nickel bubbles (Milisavljevic & Fesen 2013). This structure is probably a good representation of any realistic stripped–envelope supernova.

Gamma–ray deposition on the tail is relatively simple, being independent, for instance, of composition and relatively insensitive to density irregularities. The physics of the γ-ray deposition around the peak depends on the distribution of ^{56}Ni and ^{56}Co. Any outward "mixing" of ^{56}Ni would tend to release γ-rays more quickly and hence yield a more rapid rise, but then also lead to a more rapid late–time decay, which is already a problem with many models. There may be some turbulent "microscopic" mixing, but even Rayleigh–Taylor instabilities tend to form distinct macroscopic plumes in the non–linear limit (Hammer et al. 2010). The early deposition of gamma–rays will not be azimuthally symmetric and hence neither will be the opacity, in contrast to the conditions imposed in any spherically–symmetric model.

The current analysis suggests that the mean opacity around peak is less than frequently assumed or computed. The opacity is likely to be dependent on asymmetries that have not yet been adequately explored. The small effective opacity we derive suggests that the deposition and heating are irregular in real 3D explosions and leave substantial cold, low–opacity, mass near peak that, nevertheless, traps γ-rays on the tail.

Consideration of the nature of the opacity near peak might point the way to resolving the second dilemma that we have outlined, the self-consistency of the peak and tail properties. This perspective may also give some insight into the first dilemma, that there may be more variety in tail behavior than is clear at first blush from the peak properties. Perhaps the peak opacity and diffusion time is controlled by the fraction of the ejecta comprised of iron– and silicon–peak elements, and the mass of those elements is more uniform than the total ejecta mass.

It is striking that a substantial subset exists with similar peaks and similar tails comprising events of all stripped–envelope spectral types, SN IIb, SN Ib, and SN Ic, and with a range of photospheric velocities. Amid the diversity we emphasize, there is a uniformity that demands deeper understanding. The third dilemma, that stripped–envelope events of different spectral type, and hence different compositions, ejecta masses and perhaps energies, can have similar late–time light curves remains a challenge. We have shown that solutions can be found with appropriate choices of the mean opacity, but that choice implies a scaling with the ejecta mass and energy (Equation 14) that is far from obvious. Similar concerns remain for the fourth dilemma, how both typical and broad–line SN Ic can have similar late–time light curves. The implication is that the energy is somehow correlated with the ejected mass in an unexpected way.

Our results invoking the variation in the opacity in accord with Equation 13 imply a rather large range in ejecta masses and energies as given in Table 2 and generally larger estimates of ejecta mass and energy than other studies. Taken at face value, these results would require a substantial reconsideration of the progenitor evolution. Small ejecta masses are not compatible with the observed class of Wolf–Rayet stars. Larger ejecta masses might be. Consideration of larger mass progenitors must also confront issues of predicted rates of explosions compared to observations and issues of the sites of the explosions of the various variety of stripped–envelope events (Kelly et al. 2014). Models of the late–time spectra of SN 1985F were more compatible with the explosion of a helium core of 8 $M_\odot$ than a core of 4 $M_\odot$ (Fransson & Chevalier 1989). Some of the issues concerning the light curves of stripped–envelope supernovae might be clarified with more investigations of this type to determine the ejecta mass by independent means.

Even within the simple framework we employ here there are refinements that would make a quantitative difference. The "constants" β, C, and the "3/5" that relates the mean velocity to the photospheric velocity are functions of the density distribution and could be explored for a variety of assumed power–law exponents (Vinkó et al. 2004). The nature of positron trapping could be explored more thoroughly. In the future, better–sampled light curves from peak to tail would be valuable, and the most accurate estimates of the observed UVOIR quasi–bolometric light curve should be employed. We do not think these aspects would make a qualitative difference compared to the effects of asymmetry, ionization, and recombination we discuss here.

Clocchiatti et al. (1997) emphasized the depths of the conundrum presented by events with similar late–time tails but different spectral types and different photospheric velocities. From Equation (4), two events with the same value of $T_{0,obs}$ must have a (nearly) constant value of $M_{ej}^2/E_{ke} = 4E_{ke}/ < v^2 >^2$. The similar late–time light curves would then require some very unexpected correlation between the kinetic energy and ejecta mass and with the the mean, and hence presumably photospheric, velocity. Now, as then, the problem posed by the similar light curves and different velocities remains a challenge.

We thank Stefano Benetti, Nando Patat, Stefan Taubenberger and Stefano Valenti for sharing their bolometric light curve data, Dave Arnett and Jozsef Vinkó for a discussion of Arnett's light curve model, Maryam Modjaz, Federica Bianco and Mattias Ergon for comments, David Branch for asking a key question, and Sean Couch for a valuable perspective. This research is supported in part by NSF AST-1109801 and by the Millennium Center for Supernova Science through grant P06-045-F funded by "Programa Iniciativa Cientfica Milenio de MIDEPLAN."

REFERENCES

Arnett, W. D. 1982, Ap. J., 253, 785

Arnett, D. 1996, Supernovae and Nucleosynthesis: An Investigation of the History of Matter, from the Big Bang to the Present, Princeton: Princeton University Press, 1996.,

Barbon, R., Benetti, S., Cappellaro, E., et al. 1995, A&AS, 110, 513

Benetti, S., Turatto, M., Valenti, S., et al. 2011, Mon. Not. Royal. Ast. Soc., 411, 2726

Bianco, F. B., Modjaz, M., Hicken, M., et al. 2014, Ap. J. Supp., 213, 19

Cano, Z. 2013, Mon. Not. Royal. Ast. Soc., 434, 1098

Cano, Z., Maeda, K., & Schulze, S. 2014, Mon. Not. Royal. Ast. Soc., 438, 2924

Cappellaro, E., Mazzali, P. A., Benetti, S., et al. 1997, Astron. & Astroph., 328, 203

Chatzopoulos, E., Wheeler, J. C., & Vinko, J. 2012, Ap. J., 746, 121

Chatzopoulos, E., Wheeler, J. C., Vinko, J., Horvath, Z. L., & Nagy, A. 2013, Ap. J., 773, 76

Clocchiatti, A., Wheeler, J. C., Benetti, S., & Frueh, M. 1996, Ap. J., 459, 547

Clocchiatti, A., Wheeler, J. C., Phillips, M. M., et al. 1997, Ap. J., 483, 675

Clocchiatti, A., & Wheeler, J. C. 1997, Ap. J., 491, 375

Clocchiatti, A., Suntzeff, N. B., Phillips, M. M., et al. 2001, Ap. J., 553, 886

Clocchiatti, A., Wheeler, J. C., Kirshner, R. P., et al. 2008, Pub. Astr. Soc. Pac., 120, 290

Clocchiatti, A., Suntzeff, N. B., Covarrubias, R., & Candia, P. 2011, Astron. J., 141, 163

Dessart, L., Hillier, D. J., Li, C., & Woosley, S. 2012, Mon. Not. Royal. Ast. Soc., 424, 2139

Drout, M. R., Soderberg, A. M., Gal-Yam, A., et al. 2011, Ap. J., 741, 97

Ensman, L. M., & Woosley, S. E. 1988, Ap. J., 333, 754

Ergon, M., Sollerman, J., Fraser, M., et al. 2014, Astron. & Astroph., 562, A17

Ergon, M., Jerkstrand, A., Sollerman, J., et al. 2015, arXiv:1408.0731

Fransson, C., & Chevalier, R. A. 1989, Ap. J., 343, 323

Hammer, N. J., Janka, H.-T., Müller, E. 2010, Ap. J., 714, 1371

Höflich, P., Müller, E., & Khokhlov, A. 1993, Astron. & Astroph., 268, 570

Kelly, P. L., Filippenko, A. V., Modjaz, M., & Kocevski, D. 2014, Ap. J., 789, 23

Kleiser, I. K. W., & Kasen, D. 2014, Mon. Not. Royal. Ast. Soc., 438, 318

Lyman, J. D., Bersier, D., & James, P. A. 2014, Mon. Not. Royal. Ast. Soc., 437, 3848

Maeda, K., Mazzali, P. A., Deng, J., et al. 2003, Ap. J., 593, 931

Malesani, D., Fynbo, J. P. U., Hjorth, J., et al. 2009, Ap. J. Lett., 692, L84

Marion, G. H., Vinko, J., Kirshner, R. P., et al. 2014, Ap. J., 781, 69

Matheson, T. 2001, Pub. Astr. Soc. Pac., 113, 1155

Maund, J. R., Wheeler, J. C., Baade, D., et al. 2009, Ap. J., 705, 1139

Milisavljevic, D., & Fesen, R. A. 2013, Ap. J., 772, 134

Modjaz, M., Li, W., Butler, N., et al. 2009, Ap. J., 702, 226

Modjaz, M., Blondin, S., Kirshner, R. P., et al. 2014, Astron. J., 147, 99

Pastorello, A., Kasliwal, M. M., Crockett, R. M., et al. 2008, Mon. Not. Royal. Ast. Soc., 389, 955

Patat, F., Cappellaro, E., Danziger, J., et al. 2001, Ap. J., 555, 900

Pignata, G., Stritzinger, M., Soderberg, A., et al. 2011, Ap. J., 728, 14

Pinto, P. A., & Eastman, R. G. 2000, Ap. J., 530, 757

Piro, A. L., & Morozova, V. S. 2014, Ap. J. Lett., 792, LL11

Poznanski, D. 2013, Mon. Not. Royal. Ast. Soc., 436, 3224

Qiu, Y., Li, W., Qiao, Q., & Hu, J. 1999, Astron. J., 117, 736

Richmond, M. W., van Dyk, S. D., Ho, W., et al. 1996, Astron. J., 111, 327

Richmond, M. W., Treffers, R. R., Filippenko, A. V., et al. 1994, Astron. J., 107, 1022

Sahu, D. K., Gurugubelli, U. K., Anupama, G. C., & Nomoto, K. 2011, Mon. Not. Royal. Ast. Soc., 413, 2583

Stritzinger, M., Mazzali, P., Phillips, M. M., et al. 2009, Ap. J., 696, 713

Swartz, D. A., & Wheeler, J. C. 1991, Ap. J. Lett., 379, L13

Taddia, F., Sollerman, J., Leloudas, G., et al. 2014, arXiv:1408.4084

Taubenberger, S., Pastorello, A., Mazzali, P. A., et al. 2006, Mon. Not. Royal. Ast. Soc., 371, 1459

Tomita, H., Deng, J., Maeda, K., et al. 2006, Ap. J., 644, 400

Tsvetkov, D. Y., Volkov, I. M., Sorokina, E., et al. 2012, Peremennye Zvezdy, 32, 6

Valenti, S., Elias-Rosa, N., Taubenberger, S., et al. 2008, Ap. J. Lett., 673, L155

Valenti, S., Benetti, S., Cappellaro, E., et al. 2008, Mon. Not. Royal. Ast. Soc., 383, 1485

Valenti, S., Taubenberger, S., Pastorello, A., et al. 2012, Ap. J. Lett., 749, L28

Vinkó, J., Blake, R. M., Sárneczky, K., et al. 2004, Astron. & Astroph., 427, 453

Zhang, T., Wang, X., Zhou, X., et al. 2004, Astron. J., 128, 1857

This preprint was prepared with the AAS LaTeX macros v5.2.